1    **A series of dual-reporter vectors for ratiometric analysis of protein abundance in**

2    **plants**

3

4    Aashima Khosla[1], Cecilia Rodriguez-Furlan[1], Suraj Kapoor[2], Jaimie M. Van Norman[1],

5    David C. Nelson[1]*

6

7    [1]Department of Botany and Plant Sciences, University of California, Riverside, CA

8    92521 USA

9    [2]Department of Genetics, University of Georgia, Athens, GA 30602 USA

10

11    **ABSTRACT**

12    Ratiometric reporter systems enable comparisons of the abundance of a protein of

13    interest, or "target," relative to a reference protein. Both proteins are encoded on a single

14    transcript but are separated during translation. This arrangement bypasses the potential

15    for discordant expression that can arise when the target and reference proteins are

16    encoded by separate genes. We generated a set of 18 Gateway-compatible vectors

17    termed pRATIO that combine a variety of promoters, fluorescent and bioluminescent

18    reporters, and 2A "self-cleaving" peptides. These constructs are easily modified to

19    produce additional combinations or introduce new reporter proteins. We found that

20    mScarlet-I provides the best signal-to-noise ratio among several fluorescent reporter

21    proteins during transient expression experiments in *Nicotiana benthamiana*. Firefly and

22    Gaussia luciferase also produce high signal-to-noise in *N. benthamiana*. As proof of

23    concept, we used this system to investigate whether degradation of the receptor KAI2

24    after karrikin treatment is influenced by its subcellular localization. KAI2 is normally found

25    in the cytoplasm and the nucleus of plant cells. In *N. benthamiana,* karrikin-induced

26    degradation of KAI2 was only observed when it was retained in the nucleus. These

27    vectors are tools to easily monitor *in vivo* the abundance of a protein that is transiently

28    expressed in plants, and will be particularly useful for investigating protein turnover in

29    response to different stimuli.

30 **INTRODUCTION**

31

32 Dynamic monitoring of protein abundance *in vivo* requires an easily detectable reporter

33 system. Translational fusions of fluorescent or bioluminescent proteins to a protein of

34 interest, here referred to as a "target," are commonly used for this purpose (Bronstein et

35 al., 1994; Wood, 1995; Genové et al., 2005). Stable transformation of a host organism

36 with the target-encoding construct is typically carried out to produce a replicable and

37 relatively homogeneous reporter line, although genetic instability or gene silencing may

38 occur over subsequent generations (Vaucheret et al., 1998). The local genetic context

39 (e.g. chromatin state or nearby enhancer elements) can influence the expression of a

40 transgene. Therefore, isolation of multiple homozygous transgenic lines is typically

41 required to identify one with consistent and readily detectable expression of the target.

42 For many experiments, the cost and time involved in developing many transgenic reporter

43 lines can discourage rapid progress. This can be resolved with transient transformation

44 and expression of a reporter construct, which in plant biology research is often carried out

45 in protoplasts or *Nicotiana benthamiana* (hereafter referred to as tobacco) leaves (Yang

46 et al., 2000; Wroblewski et al., 2005). In transient expression experiments, a second

47 reporter protein that can function as a reference is useful to normalize for differences in

48 transformation efficiency or transgene expression across samples.

49

50 There are several ways to achieve a dual reporter system. Perhaps the most commonly

51 used approach is co-transformation of separate target- and reference-encoding plasmids

52 (Larrieu et al., 2015; De Sutter et al., 2005). This does not guarantee that both constructs

53 enter each cell, or that they do so with consistent proportions. Differences in the size of

54 each plasmid may also impact their relative transformation efficiencies. An improvement

55 on this method is to encode the target and reference protein on the same plasmid with

56 each regulated by its own promoter and transcriptional termination sequence (Moyle et

57 al., 2017; Koo et al., 2007). This can work well, but potential problems include the

58 increased plasmid size, the relative activity of the two promoters if they are different, and

59 recombination between promoters or terminators if they are identical.

2

60  Furthermore, the order in which the genes are expressed in the vector can influence their
61  expression levels (Halpin, 2005).

62

63  An attractive third option is to encode the target and reference protein on the same
64  transcript. This avoids variation in the relative expression of the target and reference
65  genes that may occur in different cell types or environmental conditions, as transcription
66  of both genes will be affected equally. Multicistronic gene expression can be achieved in
67  eukaryotes through incorporation of an internal ribosome entry site (IRES) or a sequence
68  encoding a 2A "self-cleaving" peptide between the target and reference genes. IRES
69  sequences produce a secondary structure in the mRNA that enables translation to occur
70  downstream (Urwin et al., 2000). The efficiency of translation for proteins encoded
71  upstream and downstream of the IRES can vary widely depending on the IRES sequence
72  selected (Urwin et al., 2002). Studies comparing the expression levels of two cDNA
73  sequences separated by an IRES have shown that genes cloned downstream of the IRES
74  were expressed at significantly lower levels (10 – 50% of the upstream gene) (Mizuguchi
75  et al., 2000). A second drawback of IRES sequences is that they are somewhat large,
76  typically ~500 to 600 bp. Because of this, 2A peptides have become a commonly used
77  alternative to produce multicistronic expression in eukaryotes.

78

79  The 2A peptide from foot-and-mouth disease virus (FMDV, "F2A") and several 2A-like
80  sequences are able to disrupt normal translation, causing a protein encoded downstream
81  of 2A to be translated separately from a protein encoded upstream (Halpin et al., 1999;
82  Ralley et al., 2004; Luke et al., 2015). This "ribosome skipping", "stop-go", or "self-
83  cleavage" effect occurs when the ribosome fails to create a glycyl-prolyl bond at the end
84  of the 2A peptide but then continues translation (Atkins et al., 2007; Doronina et al., 2008).
85  The first protein retains the majority of the 2A peptide as a C-terminal fusion, while the
86  proline residue becomes the N-terminus of the second protein (Donnelly et al., 2001c,
87  2001a; Luke and Ryan, 2018). Cleavage is thought to be caused by interaction of the
88  nascent 2A peptide with the ribosomal exit tunnel. Indeed the length of the 2A peptide
89  impacts its cleavage efficiency. A minimum of 13 amino acids of F2A are required for
90  cleavage, but longer versions are more effective. Including residues from the 1D capsid

91    peptide encoded upstream of 2A in FMDV can further increase the cleavage efficiency of

92    a 2A sequence (Donnelly et al., 2001a; Minskaia et al., 2013). While longer versions have

93    been shown to produce the most efficient cleavage, in some cases the 'remnant' 2A

94    residues appended to the C-terminus of a processed protein may hinder its activity

95    (François et al., 2004; Randall, 2004; Samalova et al., 2006). Removal of the extraneous

96    2A residues using endogenous proteases has been attempted in plant (François et al.,

97    2004) and mammalian systems (Fang et al., 2005). Conversely, when shorter 2A

98    sequences are used the C-terminal sequence of the upstream protein can impact

99    cleavage efficiency  (Minskaia et al., 2013). For shorter 2As, cleavage efficiency has been

100   improved by insertion of a flexible Gly-Ser-Gly or Ser-Gly-Ser-Gly spacer sequence

101   between the upstream protein and the 2A sequence (Fang et al., 2005; Lorens et al.,

102   2004; Szymczak et al., 2004a; Provost et al., 2007).

103

104   Several studies have used 2A peptides in dual reporter systems in plants. For example,

105   Wend *et al.* developed a degradation-based biosensor to study auxin dynamics in

106   transient expression systems (Wend et al., 2013). The chemiluminescent sensor is

107   composed of two components: a Aux/IAA degron fused to firefly luciferase (LUC) as a

108   target, and Renilla luciferase as a reference. Both components are linked by a 23 aa F2A

109   peptide. In the presence of auxin and the co-receptor F-box protein TIR1, the target is

110   degraded. Samodelov *et al.* used a similar degradation-based sensor, termed

111   StrigoQuant, to monitor strigolactone signaling in plant protoplasts (Samodelov et al.,

112   2016). This construct expressed SUPPRESSOR OF MORE AXILLARY GROWTH2-

113   LIKE6 (SMXL6) fused to LUC as a target, and Renilla luciferase as a reference.

114   Separation of the target and reference proteins was achieved by the same 23 aa F2A

115   peptide as Wend et al. The SMXL6-LUC target is degraded after strigolactone perception.

116   Samalova *et al.* utilized a fluorescent reporter to study plant membrane trafficking in both

117   transiently and stably transformed systems (Samalova et al., 2006). A 20 aa F2A peptide

118   was used to co-express a trafficked fluorescent protein marker in fixed stoichiometry with

119   a reference fluorescent protein localized to a different cellular compartment.

120 We are interested in developing a similar ratiometric system to report on signaling activity

121 in the karrikin pathway in plants. Karrikins (KARs) are a class of butenolide compounds

122 found in smoke that can stimulate seed germination and enhance the photomorphogenic

123 growth of *Arabidopsis thaliana* seedlings (Flematti et al., 2004; Nelson et al., 2009, 2010,

124 2012). KAR responses in plants require the a/b-hydrolase protein KARRIKIN

125 INSENSITIVE2 (KAI2)/HYPOSENSITIVE TO LIGHT(HTL) (Waters et al., 2012; Sun and

126 Ni, 2011). *KAI2* has roles in germination, hypocotyl elongation, drought tolerance, root

127 skewing, root hair development, and symbiotic interactions with arbuscular mycorrhizal

128 fungi (Gutjahr et al., 2015; Li et al., 2017; Villaécija-Aguilar et al., 2019; Swarbreck et al.,

129 2019). In addition to mediating KAR responses, it is thought that KAI2 recognizes an

130 unknown, endogenous signal known as KAI2 ligand (KL) (Conn and Nelson, 2015). If so,

131 KARs might be natural analogs of KL, to which some fire-following species have become

132 particularly attuned.

133

134 KAI2 works with the F-box protein MORE AXILLARY GROWTH2 (MAX2) to mediate KAR

135 responses, likely through polyubiquitination and degradation of SUPPRESSOR OF MAX2

136 1 (SMAX1) and SMAX1-LIKE2 (SMXL2) (Nelson et al., 2011; Stanga et al., 2013, 2016).

137 KAR treatment causes degradation of KAI2 protein over the course of several hours,

138 putatively as a form of negative feedback regulation (Waters et al., 2015). Proteolysis of

139 KAI2 occurs independently of MAX2 through a mechanism that is currently unknown.

140 Substitution of Ser95, one of the catalytic triad residues, with alanine renders KAI2 non-

141 functional and also prevents its degradation in the presence of KAR$_2$ (Waters et al., 2015).

142 Potentially, KAI2 degradation could be used as the basis of an *in vivo* reporter for its

143 activation. Such a bioassay could be useful in attempts to identify KL through fractionation

144 of small molecule extracts from plants.

145

146 This led us to develop a series of Gateway-compatible, plant transformation vectors for

147 ratiometric detection of a protein of interest in transient expression assays. We tested the

148 cleavage efficiency of two versions of the foot-and-mouth disease virus (FMDV) 2A

149 peptide. We compared the signal-to-noise ratio of several fluorescent and bioluminescent

150 reporters transiently expressed in *Nicotiana benthamiana* to identify those with the largest

151     potential dynamic range. Finally, as proof-of-concept, we used the ratiometric system to

152     investigate KAR-activated proteolysis of KAI2.

153

154     **RESULTS**

155

156     **Design of pRATIO vectors**

157     We constructed a series of 18 Gateway-compatible binary vectors named pRATIO that

158     encode multicistronic ratiometric reporters (Figure 1). A gene of interest can be

159     transferred readily from an entry clone into the destination vector through an LR Gateway

160     reaction (Invitrogen). The target is composed of a gene of interest that has an in-frame,

161     C-terminal fusion to a fluorescent or bioluminescent reporter gene. This is followed by a

162     2A peptide-encoding sequence and a second fluorescent or bioluminescent reporter gene

163     that serves as a reference. After the 2A peptide interrupts translation the ribosome may

164     fall off instead of resuming translation of the next coding sequence; typically this results

165     in a higher molar ratio of the first protein product vs. the second (Donnelly et al., 2001b;

166     Liu et al., 2017). Therefore, to maximize target signal, we chose to encode the target

167     protein first. Expression of the multicistronic transcript is controlled by a single promoter

168     and nopaline synthase terminator ($T_{nos}$). We selected the *35Sp* from cauliflower mosaic

169     virus, which is commonly used to drive strong expression of transgenes in plants.

170     However, *35Sp* is not equally expressed across all tissue types and can be prone to

171     silencing (Elmayan and Vaucheret, 1996). To achieve more uniform expression of the

172     ratiometric construct, several pRATIO vectors carry the *UBIQUITIN 10* promoter

173     (*UBQ10p*) from *Arabidopsis thaliana*. *UBQ10p* works well for transient expression in

174     *Arabidopsis* and tobacco tissues, and is equally useful for generating stable transgenic

175     lines (Grefen et al., 2010). Some pRATIO vectors include a nuclear localization sequence

176     (NLS) from the SV40 large T antigen that is translationally fused to the N-terminus of the

177     target. In some cases, the presence of an NLS can facilitate the detection of weak

178     fluorescent reporter signals by concentrating the signal in the nucleus (Takada and

179     Jürgens, 2007).

180    The pRATIO vectors are designed to allow for independent exchange or dropout of any

181    vector element using unique restriction endonuclease sites (Figure 1A). This can be

182    accomplished through classical restriction enzyme-mediated subcloning techniques.

183    Alternatively, a digested pRATIO vector and an insert fragment that is bordered by 15-bp

184    sequences that match the vector ends can be assembled seamlessly with a commercially

185    available enzyme mix such as NEBuilder (New England Biolabs).

186

**2A-mediated cleavage of transiently expressed reporters in tobacco**

188    The target and reference proteins are intended to separate during translation due to the

189    action of an intervening FMDV 2A (F2A) peptide. The F2A peptide itself is 19 aa long and

190    is sufficient for some degree of cleavage. However, longer versions of F2A that include

191    portions of the 1D capsid protein encoded upstream in FMDV typically produce higher

192    levels of cleavage. N-terminal extension of 2A with 5 aa of 1D improves cleavage, but

193    extension with 14, 21, and 39 aa of 1D produces complete cleavage and an equal

194    stoichiometry of the upstream and downstream translation products (Donnelly et al.,

195    2001a; Ryan et al., 1991).

196

197    The pRATIO1100 and pRATIO2100 series use a 30 aa version of F2A (11 aa of 1D plus

198    2A) while the pRATIO1200, pRATIO2200, pRATIO3200, and pRATIO4200 series use a

199    40 aa F2A sequence (21 aa of 1D plus 2A). We further modified the 40 aa F2A at its N-

200    terminus to include a 9 aa LP4 linker peptide and a flexible Gly-Ser-Gly linker, producing

201    *F2A (Figure 2A). This strategy is based upon a hybrid linker that fuses LP4, the fourth

202    linker peptide of a polyprotein precursor found in *Impatiens balsamina* seed, to a 20 aa

203    F2A peptide (Tailor et al., 1997). LP4 is post-translationally cleaved after the first or

204    second aa, enabling removal of almost the entire linker from the N-terminal protein

205    (François et al., 2002, 2004). Inclusion of a Gly-Ser-Gly linker at the N-terminal end of a

206    2A peptide can improve cleavage efficiency (Szymczak et al., 2004b; Holst et al., 2006;

207    Kim et al., 2011; Chng et al., 2015).

208

209    To compare the effectiveness of F2A and *F2A, we cloned an *Arabidopsis KAI2* cDNA

210    into pRATIO1112 and pRATIO1212. We then transiently expressed the constructs in

211  tobacco leaves via *Agrobacterium tumefaciens*-mediated transformation. These reporter

212  systems should produce a NLS-KAI2-mScarlet-I target and a Venus reference protein.

213  Fluorescence microscopy of leaf epidermal cells indicated nuclear localization of

214  mScarlet-I (Figure 2B,C). In contrast, Venus was found in both the cytoplasm and

215  nucleus, as expected for an untargeted monomeric fluorescent protein (FP). These

216  observations were consistent with successful separation of the target and reference

217  proteins.

218

219  We further examined the cleavage efficiency of F2A and *F2A through Western blot

220  analysis of total proteins extracted from transiently transformed tobacco leaves. Leaves

221  transformed with p19 alone, which suppresses gene silencing during transient

222  expression, were used as a negative control. We observed very little uncleaved protein

223  (~87 kDa) compared to NLS-KAI2-mScarlet-I (~60 kDa) and Venus (27 kDa) in leaves

224  transformed with pRATIO1112-KAI2 and pRATIO1212-KAI2 (Figure 2D). The two

225  versions of 2A peptide performed similarly well; based on the anti-Venus blot we

226  estimated cleavage efficiencies of 92% for F2A and 95% for *F2A (Figure 2E).

227

228  The LP4 linker peptide was included to further improve cleavage efficiency through post-

229  translational processing and also to remove the F2A peptide from the C-terminus of the

230  target. We noted that KAI2-mScarlet-I migrated at a slightly higher molecular weight when

231  *F2A was used compared to F2A (Figure 2D). This suggested that cleavage of LP4 might

232  not be occurring as anticipated. Therefore, we probed both samples with a monoclonal

233  antibody against 2A peptide. We found that KAI2-mScarlet-I had retained its 2A peptide

234  in pRATIO1212-KAI2 samples, indicating the LP4 linker component of *F2A was not

235  effective (Supplemental Figure 2).

236

237  All considered, *F2A did not appear to offer a clear advantage over F2A; the cleavage

238  efficiencies of these two peptides were similar and *F2A adds an extra 22 aa to the C-

239  terminus of the target protein compared to F2A. However, we noted that the abundance

240  of target and reference proteins appeared to be higher in *F2A samples than F2A samples

241  (Figure 2D). A non-specific protein bound by the GFP antibody had approximately equal

242    abundance in F2A and *F2A samples. In contrast, target and reference proteins were

243    roughly 2-fold higher in the *F2A samples than in F2A samples (Figure 2D, F). This

244    suggested that *F2A promotes more efficient translation of a polycistronic transcript than

245    F2A, and therefore may be a better choice for some applications.

246

247    **Comparison of fluorescent and luminescent reporter proteins in tobacco leaves**

248    We set out to identify reporter proteins that would be most detectable after transient

249    expression in tobacco leaves. Various FPs with different spectral properties have been

250    developed and used to analyze the dynamics of protein localization *in planta*, most

251    commonly in roots. Photosynthetic tissues, however, pose a particular challenge for

252    detecting FPs due to high background autofluorescence, e.g. from chlorophyll. We

253    selected four intrinsically bright, monomeric fluorescent reporters to test: mScarlet-I,

254    mNeonGreen, mCerulean-NLS, and Venus. We synthesized plant codon-optimized forms

255    of mScarlet-I, mNeonGreen, and mCerulean-NLS.

256

257    We selected FPs that could be paired as dual reporters with minimal spectral overlap.

258    mScarlet-I is a novel bright monomeric RFP (red fluorescent protein) with a Thr74Ile

259    mutation that results in high photostability, fast maturation (< 40 min), and a high quantum

260    yield (0.54) that is 2.5 times brighter than mCherry (Bindels et al., 2017). mScarlet-I has

261    been used in live cell imaging in Arabidopsis (Kimata et al., 2019). In the green range, we

262    chose mNeonGreen, a bright and stable green-yellow fluorescent protein derived from

263    monomerization of the tetrameric yellow fluorescent protein LanYFP (Shaner et al., 2013).

264    mNeonGreen is about 3-5 times brighter than GFP and EGFP, and its maturation time is

265    about 3-fold less than EGFP (Shaner et al., 2013; Cranfill et al., 2016; Rodriguez et al.,

266    2017; Steiert et al., 2018). Despite being a relatively new fluorescent protein, it has been

267    successfully expressed in several plant species such as *A.thaliana, N.benthamiana*, and

268    rice (Kimata et al., 2019; Kato et al., 2019; Pasin et al., 2014; Stoddard and Rolland,

269    2019; Luginbuehl et al., 2019). mCerulean is a notable *Aequorea* GFP variant that is cyan

270    in color (Rizzo et al., 2004). It is reported to be a very rapidly maturing monomer. The

271    S72A/Y145A/H148D/A206K amino acid substitutions found in mCerulean make it more

272    photostable and 2.5 times brighter than ECFP (Rizzo et al., 2004; Rizzo and Piston,

273     2005). In the yellow range, we selected Venus, an improved version of YFP (yellow

274     fluorescent protein) with a novel F46L mutation (Nagai et al., 2002). Due to its enhanced

275     brightness and fast maturation time (<20 min), Venus has been utilized in the

276     development of ratiometric sensors such as DII-VENUS and Jas9-VENUS, which monitor

277     proteins that undergo rapid turnover (Brunoud et al., 2012; Larrieu et al., 2015).

278

279     We used spectral scanning to identify excitation and emission wavelengths for each FP

280     that produced the strongest signal above background autofluorescence of tobacco

281     leaves. In some cases, these differed from the peak wavelengths identified from *in vitro*

282     studies of the FPs (Table S2). We performed tests with a KAI2 target protein to evaluate

283     the performance of pRATIO vectors containing mScarlet-I/Venus,

284     mNeonGreen/mScarlet-I, and mScarlet-I/mCerulean reporter pairs (Figure 3A). The

285     constructs were introduced into tobacco leaves by *Agrobacterium*-mediated

286     transformation. After 3 days, fluorescence signals from leaf discs were measured in a

287     microplate reader equipped with linear variable filters (Table S2). Among the four

288     fluorescent proteins, the ratio of signal to background was highest for mScarlet-I, ranging

289     from 40-fold to 156-fold (Figure 3B). The superior performance of mScarlet-I is likely a

290     combination of its exceptional brightness for a red FP and the comparably low

291     autofluorescence from tobacco leaves at its optimal excitation and emission settings

292     (Bindels et al., 2017; Thorn, 2017). Venus also worked well, with a signal intensity 46-fold

293     higher than background. In contrast, background autofluorescence was much higher

294     under mNeonGreen and mCerulean filter settings, limiting the potential dynamic range

295     and utility of these FPs in leaf tissue assays.

296

297     Bioluminescent reporter proteins potentially offer greater sensitivity and dynamic ranges

298     for quantitation than fluorescent reporters, with the drawback that they must be supplied

299     with substrates to enable detection. We selected three luciferases to test. LUC2 is an

300     improved version of the firefly luciferase isolated from *Photinus pyralis (Mašek et al.,*

301     *2013).* LUC2 requires ATP and molecular oxygen to catalyze the yellow light-emitting

302     reaction with its substrate, D-luciferin (Marques and Esteves da Silva, 2009). *P. pyralis*

303     luciferase and optimized variants of it have been used in many *in vivo* imaging

304   experiments in plants, perhaps most famously for tracking circadian clock-regulated gene
305   expression over the course of several days. A mutant form of luciferase from the
306   Japanese firefly, *Luciola cruciata,* that has a red-shifted emission spectrum (here referred
307   to as redLUC) was also chosen (Kajiyama and Nakano, 1991; Tafreshi et al., 2008).
308   redLUC also uses D-luciferin as a substrate (Branchini et al., 2005). Because of spectral
309   overlap, however, redLUC and LUC2 are not a suitable pair for dual-luciferase assays.
310   Instead, redLUC combines well in dual-luciferase assays with Gaussia Dura luciferase
311   (gLUC), a mutated blue variant of a luciferase from the marine copepod *Gaussia princeps*
312   that confers stabilized luminescence *(Welsh et al., 2009; Markova et al., 2019)*. gLUC is
313   one of the smallest and brightest luciferases currently known. It catalyzes the oxidative
314   decarboxylation of coelenterazine in an ATP-independent manner to produce blue light
315   with a peak wavelength around 480 nm (Tannous et al., 2005). Because the
316   luminescence from redLUC and gLUC can be spectrally resolved, simultaneous
317   measurement of both reporters can be accomplished without the need for two-step
318   addition of substrates or quenching.

319

320   We synthesized coding sequences for *LUC2*, *redLUC*, and *gLUC* that were codon-
321   optimized for expression in *Arabidopsis thaliana* and generated several pRATIO vectors
322   that incorporate these reporters. We tested pRATIO1231-KAI2 and pRATIO1267-KAI2,
323   which respectively use LUC2/mScarlet-I and redLUC/gLUC as target/reference reporters.
324   In comparison to FPs, firefly luciferase proteins expressed in tobacco leaves had a
325   substantially higher ratio of luminescence signal to background, due to substantially lower
326   background signals. gLUC also performed well, but had higher background signal,
327   possibly due to luciferase-independent decomposition of the coelenterazine substrate
328   (Figure 3C).

329

330   **Ratiometric analysis of KAI2 degradation in *N.benthamiana***
331   Having developed ratiometric dual-fluorescent and dual-luminescent reporters, we
332   investigated whether KAR-induced degradation of Arabidopsis KAI2 can be observed in
333   tobacco. We cloned *KAI2* and the catalytically inactive *S95A* allele of *kai2* into
334   pRATIO4212, which uses a *UBQ10* promoter and mScarlet-I/Venus reporters. Transient

335     expression of these constructs in tobacco leaf epidermal cells showed that KAI2-

336     mScarlet-I and kai2$_{S95A}$-mScarlet-I were localized to the cytoplasm and the nucleus

337     (Figure 4A). This was consistent with the subcellular localization of KAI2 in *Arabidopsis*

338     (Sun and Ni, 2011). After 12 h of treatment with 10 µM KAR$_2$, we did not observe a decline

339     in the target to reference ratio for either KAI2 or kai2$_{S95A}$ (Figure 4C). We performed

340     similar tests with pRATIO3267, which uses a *35S* promoter and redLUC/gLUC reporters.

341     Again, we did not observe a decline in the target to reference ratio after KAR$_2$ treatment

342     with either KAI2 protein (Figure 4D).

343

344     Unlike KAI2, its signaling partner MAX2 is only found in the nucleus of *Arabidopsis* cells

345     (Stirnberg et al., 2007; Shen et al., 2007). In addition, SMAX1, the target of KAI2, co-

346     localizes with TOPLESS(TPL)/TPL-RELATED(TPR) proteins in the nucleus, which is

347     consistent with the nuclear localization pattern of the homologous D53-type SMAX1-LIKE

348     (SMXL) proteins (Jiang et al., 2013; Zhou et al., 2013; Soundappan et al., 2015; Wang et

349     al., 2015; Liang et al., 2016). This led us to test whether the subcellular localization of

350     KAI2 influences its potential to be degraded after KAR treatment.

351

352     Therefore, we examined KAI2 degradation with pRATIO2212 and pRATIO1267, which

353     are respectively identical to pRATIO4212 and pRATIO3267 but add an NLS to the N-

354     terminus of the target protein. Transient expression of pRATIO4212-KAI2 and -kai2$_{S95A}$

355     in tobacco produced KAI2 fusion proteins that were exclusively localized to the nucleus.

356     In contrast to our prior results, we observed that the target to reference ratio of NLS-KAI2

357     decreased after KAR$_2$ treatment when either the dual-fluorescent or dual-luminescent

358     reporter system was used. No decline was observed for NLS-kai2$_{S95A}$ targets after KAR$_2$

359     treatment (Figure 4E,F). This is consistent with the importance of Ser95 for KAR signaling

360     and the stability of kai2$_{S95A}$ in *Arabidopsis* after KAR treatment (Waters et al., 2015). Our

361     results suggest that nuclear localization is important for KAR$_2$-induced degradation of

362     KAI2.

12

**DISCUSSION**

**Functional evaluation of the pRATIO vectors**

We developed a set of pRATIO vectors to aid studies of post-translational regulation of proteins (Figure 1). These vectors enable *in vivo* monitoring of dynamics in protein abundance in response to applied stimuli. These assays can be carried out rapidly in transient expression systems. Importantly, pRATIO vectors can normalize differences in transformation efficiency or transgene expression across samples by simultaneously expressing a reference protein from the same transcript as a target protein of interest. This is made possible by the use of a short "self-cleaving" F2A peptide derived from FMDV. To date, there has not been a comprehensive study that compares the cleavage efficiencies of different 2A peptides in plants. Of the various 2A and 2A-like peptides, the most widely used 2A sequence in plants is F2A (Halpin et al., 1999; El Amrani et al., 2004; Samalova et al., 2006; François et al., 2004; Ma and Mitra, 2002; Burén et al., 2012). We tested two long versions of the F2A peptide, one of which included a putative protease cleavage site that proved to be ineffective. We found that F2A and *F2A have similarly high cleavage efficiencies but that *F2A allows better protein expression (Figure 2). We identified the fluorescent proteins mScarlet-I and Venus, and the bioluminescent proteins redLUC and gLUC, as particularly useful reporter pairs for ratiometric target detection in tobacco leaves (Figure 3). Their superior performance is likely due to the low background signal from green plant tissue at their detection filter settings. The pRATIO vectors have a modular configuration in which the promoter, Gateway cassette, 2A peptide, reporters are flanked by unique restriction endonuclease cleavage sites (Figure 1). This makes further modification of pRATIO vectors to fit specific experimental needs easy to accomplish.

We found that *Arabidopsis* KAI2 was degraded in tobacco following KAR$_2$ treatment, demonstrating that this response is conserved between the two species (Figure 4; Waters et al., 2015). KAR-induced degradation of KAI2 was only observed when KAI2 was retained in the nucleus. Interestingly, MAX2 and SMAX1, the signaling partners of KAI2, are nuclear proteins. Although KAI2 degradation is known to be MAX2-independent,

13

394     future work should investigate whether it depends on KAI2 association with SMAX1 in the

395     nucleus.

396

**Limitations of the pRATIO system**

398     We note three important limitations when using the pRATIO vectors. First, an appropriate

399     filter set is critical to maximize the signal and reduce spectral overlap between fluorescent

400     proteins (Tables S2, S3). We used spectral scanning to identify optimal excitation and

401     emission settings for each fluorophore in green leaves. However, when typical filter

402     settings for GFP (excitation 488 nm; emission 507 nm), mCherry (excitation 587 nm;

403     emission 610 nm), and CFP (excitation 433 nm; emission 475 nm) were used to detect

404     mNeonGreen, mScarlet-I, and mCerulean, respectively, the fluorescence signal over

405     background was greatly diminished (data not shown). Thus, the use of some of these

406     reporters may be limited by the availability of a multi-mode plate reader that can set

407     continuously adjustable wavelengths and bandwidths for excitation and emission.

408

409     Second, although our *F2A sequence produced efficient cleavage and stronger

410     expression of target and reference proteins than F2A, it was not removed from the target

411     post-translationally as anticipated. It is possible that the C-terminal extension may

412     interfere with the function of a target protein or with the activity of reporter proteins. This

413     may not pose a significant problem for pRATIO vectors, as we were able to detect all

414     reporter proteins effectively (Supplemental Figure 1). In cases where this is a problem,

415     however, a better alternative to *F2A may be IntF2A, a fusion of an Ssp DnaE mini-intein

416     variant to a long 58 aa F2A peptide (Zhang et al., 2017). IntF2A is rapidly and efficiently

417     removed from the C-terminal end of a fusion protein through the hyper-N-terminal auto-

418     cleaving action of the intein after translation. IntF2 has been shown to be processed

419     efficiently in multiple organs of transgenic *Nicotiana tabacum*, and in transiently

420     transformed *N. benthamiana* and lettuce (Zhang et al., 2017).

421

422     Third, we found pRATIO vectors to be useful in transient expression assays, but we were

423     unable to detect the Venus or mCerulean-NLS reference proteins in transgenic

424     *Arabidopsis thaliana* lines carrying pRATIO2212-KAI2 or pRATIO2214-KAI2 by

425    fluorescence microscopy (Supplemental Figure 3). One likely explanation is that the

426    ribosome does not always continue translation after disruption of the glycyl-prolyl bond at

427    the end of the 2A peptide and instead drops off (Ryan et al., 1999; Donnelly et al., 2001a;

428    de Felipe et al., 2003; Liu et al., 2017). The high level of transient expression that can be

429    achieved in tobacco may overcome an inefficiency in translating the reference protein.

430    Notably, the 2A-dependent ratiometric sensors for auxin and strigolactone have only been

431    deployed in transient expression experiments in protoplasts, raising the question of

432    whether they are effective as stable transgenes (Wend et al., 2013; Samodelov et al.,

433    2016).

434

435    Alternatively, 2A peptides may have different effects in different species, depending on

436    how they interact with the ribosome.  For example, the cleavage efficiencies of the 2A

437    peptide from FMDV have ranged from 40% to 90% to nearly 100% (Donnelly et al., 2001a;

438    Szymczak et al., 2004b; Kim et al., 2011). This variability is likely due to differences in

439    experimental conditions, including the use of different model organisms. 2A variants

440    found in other viruses, such as equine rhinitis A virus 2A (E2A), porcine teschovirus-1 2A

441    (P2A), thosea asigna virus 2A (T2A), can have different activities in a given system (Ryan

442    et al., 1991; Donnelly et al., 2001a; Szymczak and Vignali, 2005). The 22 aa version of

443    F2A produces the least efficient cleavage of four 2A peptides tested in human cell lines,

444    zebrafish embryos, and mouse liver. P2A is most effective, in some cases producing more

445    than twice the cleavage efficiency of F2A (Kim et al., 2011). It is possible that other 2A

446    forms may be more effective than F2A at inducing stop-and-go translation in transgenic

447    plants. It will be interesting to determine whether there is a tradeoff between cleavage

448    efficiency and the frequency of continued translation of the second coding sequence. We

449    propose that a high cleavage efficiency should be prioritized for accurate monitoring of

450    target/reference ratios.

451

452    **Future applications for ratiometric reporters**

453    There are a number of potential applications for controlled co-expression of target and

454    reference proteins from a single polycistronic mRNA, particularly if the reference protein

455    can be detected in stably transformed plants. For example, the *35S* or *UBQ10* promoters

456    in a pRATIO construct could be replaced with a native promoter and coding sequence for

457    a gene of interest. This would potentially enable monitoring of the protein distribution and

458    transcriptional pattern of a gene in a single construct by visualizing the target and

459    reference reporters, respectively. In addition to revealing differences in localization

460    patterns, such a system could be used to simultaneously examine changes in gene

461    expression at the transcript and protein levels. In the case of understanding the nature of

462    KL, we anticipate development of a reliable reporter of KAI2 signaling activity will facilitate

463    KL identification through bioassay-guided fractionation. Alternatively, a ratiometric

464    reporter of KAI2 signaling may enable genetic screens for KL-deficient or -overproducing

465    mutants.

466

467    **SUPPLEMENTAL DATA**

468

469    **Supplemental Figure 1.** Fluorescence microscopy images showing the expression of

470    reference proteins in tobacco epidermal cells.

471    **Supplemental Figure 2**. Western blot analysis revealing cleavage efficiency in the 2As

472    in tobacco epidermal cells.

473    **Supplemental Figure 3.** Reference protein is undetectable in *Arabidopsis thaliana*.

474    **Supplemental Table 1.** List of vectors in the pRATIO series.

475    **Supplemental Table 2.** Fluorescent proteins (FPs) used in this study.

476    **Supplemental Table 3.** Luciferases used in this study.

477    **Supplemental Table 4.** Primers used in this study.

478    **Supplemental Table 5.** GenBank accession numbers for the pRATIO vectors.

479

480    **ACKNOWLEDGEMENTS**

481

**AUTHOR CONTRIBUTIONS**

Project and experimental design by AK and DCN. Experiments were carried out by AK, SK, and CR. All authors contributed to data analysis and interpretation. Figure preparation by AK and DCN. Manuscript preparation by AK, JMVN, and DCN.

**METHODS**

**Construction of plant transformation vectors**

**Biological components**

The plant codon optimized coding sequence of *mScarlet-I, LUC2, mCeruelan-NLS,* and *redLUC-\*F2A-gLUC* were synthesized in pUC57 cloning vectors (Genscript) using *KpnI - SacI*, *ApaI-MluI*, *KpnI-SacI*, and *MluI-SacI* restriction sites, respectively. The *Arabidopsis UBQ10* promoter was derived from pUBQ10:YFP-GW plasmid (Michniewicz et al., 2015), plant codon optimized *mNeonGreen* from pMCS:mNeonGreen-GW plasmid (Lucia Strader, Washington University), and NLS from SV40 large T antigen.

pUC57-mScarlet-I: mScarlet-I in pUC57

pUC57-mCerulean: mCerulean-NLS in pUC57

pUC57-LUC2: LUC2 in pUC57

pUC57-redgLUC:  redLUC-P-2A-gLUC in pUC57

pUC57-mNeonGreen:  pUBQ10-NLS-GW-mNeonGreen-F2A-mCherry in pUC57

pUC57-mNeonGreen was used as a template to generate pRATIO2131. mScarlet-I was excised from pUC57-mScarlet-I using *KpnI-SacI* and inserted into the corresponding site of pUC57-mNeonGreen to generate pUC2131. The *HindIII-SacI* fragment of the resulting plasmid was ligated into the same sites of pGWB401 (Nakagawa et al., 2007) to generate pRATIO2131.

To create pRATIO2112, the coding sequence of *Venus* was amplified from pCN-SANB-nu3V (Wolfgang Busch, Salk Institute) using primers that introduce 5' *KpnI* site and a 3'

17

517  *SacI* site. The PCR product was digested with *KpnI-SacI* and inserted into *KpnI-SacI*

518  digested pUC57-mNeonGreen. The coding sequence of *mScarlet-I* was amplified from

519  pUC57-mScarlet-I with gene specific primers introducing a 5' *ApaI* site and 3' *Mlu*I site.

520  The resulting PCR product was digested with *ApaI-MluI* and inserted into the

521  corresponding site of pUC57-mNeonGreen to generate pUC2112. The resulting

522  pUBQ10-NLS-GW-mScarlet-I-F2A-Venus was released from pUC57 using *HindIII-SacI*

523  and inserted into *HindIII-SacI* digested pGWB401. Oligonucleotides used for PCR

524  amplifications are listed in Table S4.

525  To generate pRATIO2151, LUC2 was excised from pUC57-LUC2 using *ApaI-MluI* and

526  cloned into *ApaI-MluI* digested pUC2131 to generate pUC2151. The *HindIII-SacI*

527  fragment of the resulting plasmid was ligated into the same sites of pGWB401 to generate

528  pRATIO2151.

529  To create pRATIO1112, pUBQ10-NLS-GW-mScarlet-I-F2A-Venus was released from

530  pUC2112 using *XbaI* and *SacI* restriction enzymes and cloned into *XbaI - SacI* digested

531  pGBW402 (Nakagawa et al., 2007). pRATIO1131 and 1151 were made in a similar

532  fashion using pUC2131 and pUC2151 as template, respectively.

533  *F2A was excised from pUC57-redgLUC using *MluI* and *KpnI,* and subcloned into the

534  same sites of pRATIO1112 and 1151 to create pRATIO1212 and 1251, respectively.

535  To generate pRATIO1267, pUC57-redgLUC was digested with *ApaI* and *SacI* and

536  inserted into the corresponding site of pRATIO1212.

537  To construct pRATIO2212, pRATIO2251, and pRATIO2231, *F2A was released from

538  pUC57-redgLUC using *MluI* and *KpnI* and ligated into the corresponding sites of

539  pRATIO2112, 2151, and 2231, respectively.

540  To create pRATIO2214, mCerulean-NLS was excised from pUC57-mCerulean using

541  *KpnI* and *SacI* and ligated into *KpnI-SacI* digested pRATIO2212.

542  To construct the no NLS versions of pRATIO, NLS sequence was removed by digesting

543  pRATIO1212, pRATIO2212-2231 with *XbaI-SpeI*, followed by self-ligation to generate

544  pRATIO3212, pRATIO4212-4231, respectively.

18

**Transient expression in *N.benthamiana***

*Nicotiana benthamiana* were grown in soil in a growth room at 22°C under long day conditions (16/8 hr light dark cycle). *N. benthamiana* leaves (3 weeks old) were infiltrated with *A. tumefaciens* strain GV3101 harboring pRATIO-KAI2 fusion vectors. GV3101 cells were grown in 10 ml LB broth with antibiotics overnight at 28°C and then pelleted at 2,500 x$g$ for 10 min. Cells were then washed in 10 ml of infiltration medium (10 mM MES pH 5.7, 10 mM $MgCl_2$ and 150 μM acetosyringone), centrifuged again at 2,500 x$g$ for 5 min and resuspended in infiltration medium at an $OD_{600}$ of 0.2. The *Agrobacterium* solution was infiltrated in the abaxial surface of the leaf using a 1 ml syringe without a needle. After infiltration plants were placed under normal light conditions and leaves were collected after 72 hours for further analysis.

**Degradation assays in tobacco**

To generate pRATIO vectors with KAI2 and $kai2_{S95A}$ fusions, full length *KAI2* coding sequence was amplified from Col-0 cDNA and inserted into Gateway entry vector pDONR207. The resulting entry clone was then moved to the pRATIO destination vectors by gateway LR reaction. The $kai2_{S95A}$ mutant was generated with Infusion on *KAI2* entry clone described above, and subsequently recombined with pRATIO vectors.

To perform degradation assays, leaf discs were excised 3 days post infiltration and incubated at RT for 12 hr in the presence or absence of 10 μM $KAR_2$ or 0.02% acetone control. mScarlet-I (target) and Venus (reference) were excited at 560 ± 10 nm and 497 ± 15 nm in a CLARIOstar plate reader (BMG Labtech, Ortenberg, Germany). Emission was recorded at 595 ± 10 nm (mScarlet-I) and 540 ± 20 nm (Venus) using black 96-well plates (Costar). Degradation was quantified as mScarlet-I/Venus fluorescence intensity ratios after background subtraction using p19 transformed leaf disc.

For luminescence-based degradation assay, redLUC and gLUC were detected at 640 ± 10 nm and 480 ± 40 nm, respectively using white 96-well plates (PerkinElmer).

19

**Fluorescence and luminescence measurements**

Fluorescence and luminescence were measured off-line using the CLARIOstar plate reader (BMG Labtech, Ortenberg, Germany). Fluorescence intensity was measured in well scan mode of density 9×9 (9 points per well) in black, flat bottom plates. For mScarlet-I, Venus, mNeonGreen, and mCerulean detection, the optic settings (excitation, dichroic, and emission) to obtain best signal to noise ratio are listed in Table S2. Luminescence was measured in endpoint mode in white, flat bottom plates (costar). Table S3 shows the optimal filters to detect LUC2, redLUC, and gLUC signals in *N.benthamiana*.

Tobacco leaf discs were imaged 3 days after agroinfiltration on Keyence BZ-X710 epi fluorescence microscope. Fluorescence was observed using the RFP filter setting (Ex 470/40 nm, Em 535/50nm) to detect mScarlet-I.

**Protein extraction and western blot analysis**

Transformed tobacco leaves were ground in liquid nitrogen and then resuspended hot SDS-sample buffer (100 mM Tris-HCl, pH 6.8, 2% SDS, 20% glycerol, 100 mM DTT, and 0.004% bromophenol blue, 0.48 g Urea per ml). Samples were then cleaned by centrifugation at 10,000 xg at room temperature. For western blotting analysis, samples were separated on SDS-PAGE and the proteins were transferred onto PVDF membrane. Subsequently, the membrane was probed with the indicated primary antibody (rabbit anti-GFP [1:1500, Abcam, #ab290], mouse anti-RFP [1:1000, Chromotek, #6G6], and mouse anti-2A [1:1000, Sigma, #3H4]), washed with TBST, and probed with HRP-conjugated mouse anti-rabbit (1:10,000, Genscript, #A01856) and horse anti-mouse (1:5000, Cell Signaling, #7076). Blots were developed using an Azure Radiance Plus chemiluminescent substrate (#AC2102).

## REFERENCES

Atkins, J.F., Wills, N.M., Loughran, G., Wu, C.-Y., Parsawar, K., Ryan, M.D., Wang, C.-H., and Nelson, C.C. (2007). A case for "StopGo": Reprogramming translation to augment codon meaning of GGN by promoting unconventional termination (Stop) after addition of glycine and then allowing continued translation (Go). RNA 13: 803–810.

Bindels, D.S., Haarbosch, L., van Weeren, L., Postma, M., Wiese, K.E., Mastop, M., Aumonier, S., Gotthard, G., Royant, A., Hink, M.A., and Gadella, T.W.J., Jr (2017). mScarlet: a bright monomeric red fluorescent protein for cellular imaging. Nat. Methods 14: 53–56.

Branchini, B.R., Southworth, T.L., Khattak, N.F., Michelini, E., and Roda, A. (2005). Red- and green-emitting firefly luciferase mutants for bioluminescent reporter applications. Anal. Biochem. 345: 140–148.

Bronstein, I., Fortin, J., Stanley, P.E., Stewart, G.S., and Kricka, L.J. (1994). Chemiluminescent and bioluminescent reporter gene assays. Anal. Biochem. 219: 169–181.

Brunoud, G., Wells, D.M., Oliva, M., Larrieu, A., Mirabet, V., Burrow, A.H., Beeckman, T., Kepinski, S., Traas, J., Bennett, M.J., and Vernoux, T. (2012). A novel sensor to map auxin response and distribution at high spatio-temporal resolution. Nature 482: 103–106.

Burén, S., Ortega-Villasante, C., Otvös, K., Samuelsson, G., Bakó, L., and Villarejo, A. (2012). Use of the foot-and-mouth disease virus 2A peptide co-expression system to study intracellular protein trafficking in Arabidopsis. PLoS One 7: e51973.

Chng, J., Wang, T., Nian, R., Lau, A., Hoi, K.M., Ho, S.C.L., Gagnon, P., Bi, X., and Yang, Y. (2015). Cleavage efficient 2A peptides for high level monoclonal antibody expression in CHO cells. mAbs 7: 403–412.

Conn, C.E. and Nelson, D.C. (2015). Evidence that KARRIKIN-INSENSITIVE2 (KAI2) Receptors may Perceive an Unknown Signal that is not Karrikin or Strigolactone. Front. Plant Sci. 6: 1219.

Cranfill, P.J., Sell, B.R., Baird, M.A., Allen, J.R., Lavagnino, Z., de Gruiter, H.M., Kremers, G.-J., Davidson, M.W., Ustione, A., and Piston, D.W. (2016). Quantitative assessment of fluorescent proteins. Nat. Methods 13: 557–562.

De Sutter, V., Vanderhaeghen, R., Tilleman, S., Lammertyn, F., Vanhoutte, I., Karimi, M., Inzé, D., Goossens, A., and Hilson, P. (2005). Exploration of jasmonate signalling via automated and standardized transient expression assays in tobacco cells. Plant J. 44: 1065–1076.

Donnelly, M.L.L., ten Dam, E., Gani, D., Luke, G., Ryan, M.D., Mendoza, H., and Hughes, L.E. (2001a). The "cleavage" activities of foot-and-mouth disease virus 2A site-directed mutants and naturally occurring "2A-like" sequences. Journal of General Virology 82: 1027–1041.

Donnelly, M.L.L., Luke, G., Mehrotra, A., Li, X., Hughes, L.E., Gani, D., and Ryan, M.D. (2001b). Analysis of the aphthovirus 2A/2B polyprotein "cleavage"mechanism indicates not a proteolytic reaction, but a novel translational effect: a putative ribosomal "skip." J. Gen. Virol. 82: 1013–1025.

Donnelly, M.L.L., Ryan, M.D., Mehrotra, A., Gani, D., Hughes, L.E., Luke, G., and Li, X. (2001c).

638    Analysis of the aphthovirus 2A/2B polyprotein "cleavage" mechanism indicates not a
639    proteolytic reaction, but a novel translational effect: a putative ribosomal "skip." Journal of
640    General Virology 82: 1013–1025.

641 Doronina, V.A., Wu, C., de Felipe, P., Sachs, M.S., Ryan, M.D., and Brown, J.D. (2008). Site-
642    specific release of nascent chains from ribosomes at a sense codon. Mol. Cell. Biol. 28:
643    4227–4239.

644 El Amrani, A., Barakate, A., Askari, B.M., Li, X., Roberts, A.G., Ryan, M.D., and Halpin, C.
645    (2004). Coordinate expression and independent subcellular targeting of multiple proteins
646    from a single transgene. Plant Physiol. 135: 16–24.

647 Elmayan, T. and Vaucheret, H. (1996). Expression of single copies of a strongly expressed 35S
648    transgene can be silenced post-transcriptionally. Plant J. 9: 787–797.

649 Fang, J., Qian, J.-J., Yi, S., Harding, T.C., Tu, G.H., VanRoey, M., and Jooss, K. (2005). Stable
650    antibody expression at therapeutic levels using the 2A peptide. Nat. Biotechnol. 23: 584–
651    590.

652 de Felipe, P., Hughes, L.E., Ryan, M.D., and Brown, J.D. (2003). Co-translational,
653    intraribosomal cleavage of polypeptides by the foot-and-mouth disease virus 2A peptide. J.
654    Biol. Chem. 278: 11441–11448.

655 Flematti, G.R., Ghisalberti, E.L., Dixon, K.W., and Trengove, R.D. (2004). A compound from
656    smoke that promotes seed germination. Science 305: 977.

657 François, I.E.J.A., De Bolle, M.F.C., Dwyer, G., Goderis, I.J.W.M., Woutors, P.F.J., Verhaert,
658    P.D., Proost, P., Schaaper, W.M.M., Cammue, B.P.A., and Broekaert, W.F. (2002).
659    Transgenic expression in Arabidopsis of a polyprotein construct leading to production of
660    two different antimicrobial proteins. Plant Physiol. 128: 1346–1358.

661 François, I.E.J.A., Isabelle E J, Van Hemelrijck, W., Aerts, A.M., Wouters, P.F.J., Proost, P.,
662    Broekaert, W.F., and Cammue, B.P.A. (2004). Processing in Arabidopsis thaliana of a
663    heterologous polyprotein resulting in differential targeting of the individual plant defensins.
664    Plant Science 166: 113–121.

665 Genové, G., Glick, B.S., and Barth, A.L. (2005). Brighter reporter genes from multimerized
666    fluorescent proteins. Biotechniques 39: 814, 816, 818 passim.

667 Grefen, C., Donald, N., Hashimoto, K., Kudla, J., Schumacher, K., and Blatt, M.R. (2010). A
668    ubiquitin-10 promoter-based vector set for fluorescent protein tagging facilitates temporal
669    stability and native protein distribution in transient and stable expression studies. Plant J.
670    64: 355–365.

671 Gutjahr, C. et al. (2015). Rice perception of symbiotic arbuscular mycorrhizal fungi requires the
672    karrikin receptor complex. Science 350: 1521–1524.

673 Halpin, C. (2005). Gene stacking in transgenic plants--the challenge for 21st century plant
674    biotechnology. Plant Biotechnol. J. 3: 141–155.

675 Halpin, C., Cooke, S.E., Barakate, A., El Amrani, A., and Ryan, M.D. (1999). Self-processing
676    2A-polyproteins--a system for co-ordinate expression of multiple proteins in transgenic

677     plants. Plant J. 17: 453–459.

678     Holst, J., Szymczak-Workman, A.L., Vignali, K.M., Burton, A.R., Workman, C.J., and Vignali,
679          D.A.A. (2006). Generation of T-cell receptor retrogenic mice. Nat. Protoc. 1: 406–417.

680     Jiang, L. et al. (2013). DWARF 53 acts as a repressor of strigolactone signalling in rice. Nature
681          504: 401–405.

682     Kajiyama, N. and Nakano, E. (1991). Isolation and characterization of mutants of firefly
683          luciferase which produce different colors of light. Protein Eng. 4: 691–693.

684     Kato, H. et al. (2019). Design principles of a minimal auxin response system. bioRxiv: 760876.

685     Kimata, Y., Kato, T., Higaki, T., Kurihara, D., Yamada, T., Segami, S., Morita, M.T., Maeshima,
686          M., Hasezawa, S., Higashiyama, T., Tasaka, M., and Ueda, M. (2019). Polar vacuolar
687          distribution is essential for accurate asymmetric division of Arabidopsis zygotes. Proc. Natl.
688          Acad. Sci. U. S. A. 116: 2338–2343.

689     Kim, J.H., Lee, S.-R., Li, L.-H., Park, H.-J., Park, J.-H., Lee, K.Y., Kim, M.-K., Shin, B.A., and
690          Choi, S.-Y. (2011). High cleavage efficiency of a 2A peptide derived from porcine
691          teschovirus-1 in human cell lines, zebrafish and mice. PLoS One 6: e18556.

692     Koo, J., Kim, Y., Kim, J., Yeom, M., Lee, I.C., and Nam, H.G. (2007). A GUS/luciferase fusion
693          reporter for plant gene trapping and for assay of promoter activity with luciferin-dependent
694          control of the reporter protein stability. Plant Cell Physiol. 48: 1121–1131.

695     Larrieu, A. et al. (2015). A fluorescent hormone biosensor reveals the dynamics of jasmonate
696          signalling in plants. Nat. Commun. 6: 6043.

697     Liang, Y., Ward, S., Li, P., Bennett, T., and Leyser, O. (2016). SMAX1-LIKE7 Signals from the
698          Nucleus to Regulate Shoot Development in Arabidopsis via Partially EAR Motif-
699          Independent Mechanisms. Plant Cell 28: 1581–1601.

700     Liu, Z., Chen, O., Wall, J.B.J., Zheng, M., Zhou, Y., Wang, L., Ruth Vaseghi, H., Qian, L., and
701          Liu, J. (2017). Systematic comparison of 2A peptides for cloning multi-genes in a
702          polycistronic vector. Sci. Rep. 7: 2193.

703     Li, W., Nguyen, K.H., Chu, H.D., Van Ha, C., Watanabe, Y., Osakabe, Y., Leyva-González,
704          M.A., Sato, M., Toyooka, K., Voges, L., and Others (2017). The karrikin receptor KAI2
705          promotes drought resistance in Arabidopsis thaliana. PLoS Genet. 13: e1007076.

706     Lorens, J.B., Pearsall, D.M., Swift, S.E., Peelle, B., Armstrong, R., Demo, S.D., Ferrick, D.A.,
707          Hitoshi, Y., Payan, D.G., and Anderson, D. (2004). Stable, stoichiometric delivery of diverse
708          protein functions. J. Biochem. Biophys. Methods 58: 101–110.

709     Luginbuehl, L.H., El-Sharnouby, S., Wang, N., and Hibberd, J.M. (2019). Fluorescent reporters
710          for functional analysis in rice leaves. bioRxiv: 649160.

711     Luke, G.A., Roulston, C., Tilsner, J., and Ryan, M.D. (2015). Growing Uses of 2A in Plant
712          Biotechnology. Biotechnology.

713     Luke, G.A. and Ryan, M.D. (2018). Using the 2A Protein Coexpression System: Multicistronic
714          2A Vectors Expressing Gene(s) of Interest and Reporter Proteins. Methods Mol. Biol. 1755:

715        31–48.

716    Ma, C. and Mitra, A. (2002). Expressing multiple genes in a single open reading frame with the
717        2A region of foot-and-mouth disease virus as a linker. Mol. Breed. 9: 191–199.

718    Markova, S.V., Larionova, M.D., and Vysotski, E.S. (2019). Shining Light on the Secreted
719        Luciferases of Marine Copepods: Current Knowledge and Applications. Photochem.
720        Photobiol. 95: 705–721.

721    Marques, S.M. and Esteves da Silva, J.C.G. (2009). Firefly bioluminescence: a mechanistic
722        approach of luciferase catalyzed reactions. IUBMB Life 61: 6–17.

723    Mašek, T., Vopalenský, V., and Pospíšek, M. (2013). The Luc2 gene enhances reliability of
724        bicistronic assays. Open Life Sciences 8.

725    Michniewicz, M., Frick, E.M., and Strader, L.C. (2015). Gateway-compatible tissue-specific
726        vectors for plant transformation. BMC Res. Notes 8: 63.

727    Minskaia, E., Nicholson, J., and Ryan, M.D. (2013). Optimisation of the foot-and-mouth disease
728        virus 2A co-expression system for biomedical applications. BMC Biotechnol. 13: 67.

729    Mizuguchi, H., Xu, Z., Ishii-Watabe, A., Uchida, E., and Hayakawa, T. (2000). IRES-dependent
730        second gene expression is significantly lower than cap-dependent first gene expression in a
731        bicistronic vector. Mol. Ther. 1: 376–382.

732    Moyle, R.L., Carvalhais, L.C., Pretorius, L.-S., Nowak, E., Subramaniam, G., Dalton-Morgan, J.,
733        and Schenk, P.M. (2017). An Optimized Transient Dual Luciferase Assay for Quantifying
734        MicroRNA Directed Repression of Targeted Sequences. Front. Plant Sci. 8: 1631.

735    Nagai, T., Ibata, K., Park, E.S., Kubota, M., Mikoshiba, K., and Miyawaki, A. (2002). A variant of
736        yellow fluorescent protein with fast and efficient maturation for cell-biological applications.
737        Nat. Biotechnol. 20: 87–90.

738    Nakagawa, T., Kurose, T., Hino, T., Tanaka, K., Kawamukai, M., Niwa, Y., Toyooka, K.,
739        Matsuoka, K., Jinbo, T., and Kimura, T. (2007). Development of series of gateway binary
740        vectors, pGWBs, for realizing efficient construction of fusion genes for plant transformation.
741        J. Biosci. Bioeng. 104: 34–41.

742    Nelson, D.C., Flematti, G.R., Ghisalberti, E.L., Dixon, K.W., and Smith, S.M. (2012). Regulation
743        of seed germination and seedling growth by chemical signals from burning vegetation.
744        Annu. Rev. Plant Biol. 63: 107–130.

745    Nelson, D.C., Flematti, G.R., Riseborough, J.-A., Ghisalberti, E.L., Dixon, K.W., and Smith, S.M.
746        (2010). Karrikins enhance light responses during germination and seedling development in
747        Arabidopsis thaliana. Proc. Natl. Acad. Sci. U. S. A. 107: 7095–7100.

748    Nelson, D.C., Riseborough, J.-A., Flematti, G.R., Stevens, J., Ghisalberti, E.L., Dixon, K.W., and
749        Smith, S.M. (2009). Karrikins discovered in smoke trigger Arabidopsis seed germination by
750        a mechanism requiring gibberellic acid synthesis and light. Plant Physiol. 149: 863–873.

751    Nelson, D.C., Scaffidi, A., Dun, E.A., Waters, M.T., Flematti, G.R., Dixon, K.W., Beveridge, C.A.,
752        Ghisalberti, E.L., and Smith, S.M. (2011). F-box protein MAX2 has dual roles in karrikin and
753        strigolactone signaling in Arabidopsis thaliana. Proc. Natl. Acad. Sci. U. S. A. 108: 8897–

754    8902.

755    Pasin, F., Kulasekaran, S., Natale, P., Simón-Mateo, C., and García, J.A. (2014). Rapid
756        fluorescent reporter quantification by leaf disc analysis and its application in plant-virus
757        studies. Plant Methods 10: 22.

758    Provost, E., Rhee, J., and Leach, S.D. (2007). Viral 2A peptides allow expression of multiple
759        proteins from a single ORF in transgenic zebrafish embryos. Genesis 45: 625–629.

760    Ralley, L., Enfissi, E.M.A., Misawa, N., Schuch, W., Bramley, P.M., and Fraser, P.D. (2004).
761        Metabolic engineering of ketocarotenoid formation in higher plants. The Plant Journal 39:
762        477–486.

763    Randall, J. (2004). Co-ordinate expression of beta;- and delta;-zeins in transgenic tobacco.
764        Plant Science.

765    Rizzo, M.A. and Piston, D.W. (2005). High-contrast imaging of fluorescent protein FRET by
766        fluorescence polarization microscopy. Biophys. J. 88: L14–6.

767    Rizzo, M.A., Springer, G.H., Granada, B., and Piston, D.W. (2004). An improved cyan
768        fluorescent protein variant useful for FRET. Nat. Biotechnol. 22: 445–449.

769    Rodriguez, E.A., Campbell, R.E., Lin, J.Y., Lin, M.Z., Miyawaki, A., Palmer, A.E., Shu, X.,
770        Zhang, J., and Tsien, R.Y. (2017). The Growing and Glowing Toolbox of Fluorescent and
771        Photoactive Proteins. Trends Biochem. Sci. 42: 111–129.

772    Ryan, M.D., Donnelly, M., Lewis, A., Mehrotra, A.P., Wilkie, J., and Gani, D. (1999). A Model for
773        Nonstoichiometric, Cotranslational Protein Scission in Eukaryotic Ribosomes. Bioorg.
774        Chem. 27: 55–79.

775    Ryan, M.D., King, A.M., and Thomas, G.P. (1991). Cleavage of foot-and-mouth disease virus
776        polyprotein is mediated by residues located within a 19 amino acid sequence. J. Gen. Virol.
777        72 ( Pt 11): 2727–2732.

778    Samalova, M., Fricker, M., and Moore, I. (2006). Ratiometric Fluorescence-Imaging Assays of
779        Plant Membrane Traffic Using Polyproteins. Traffic 7: 1701–1723.

780    Samodelov, S.L., Beyer, H.M., Guo, X., Augustin, M., Jia, K.-P., Baz, L., Ebenhöh, O., Beyer,
781        P., Weber, W., Al-Babili, S., and Zurbriggen, M.D. (2016). StrigoQuant: A genetically
782        encoded biosensor for quantifying strigolactone activity and specificity. Sci Adv 2:
783        e1601266.

784    Shaner, N.C., Lambert, G.G., Chammas, A., Ni, Y., Cranfill, P.J., Baird, M.A., Sell, B.R., Allen,
785        J.R., Day, R.N., Israelsson, M., Davidson, M.W., and Wang, J. (2013). A bright monomeric
786        green fluorescent protein derived from Branchiostoma lanceolatum. Nat. Methods 10: 407–
787        409.

788    Shen, H., Luong, P., and Huq, E. (2007). The F-box protein MAX2 functions as a positive
789        regulator of photomorphogenesis in Arabidopsis. Plant Physiol. 145: 1471–1483.

790    Soundappan, I., Bennett, T., Morffy, N., Liang, Y., Stanga, J.P., Abbas, A., Leyser, O., and
791        Nelson, D.C. (2015). SMAX1-LIKE/D53 Family Members Enable Distinct MAX2-Dependent
792        Responses to Strigolactones and Karrikins in Arabidopsis. Plant Cell 27: 3143–3159.

793    Stanga, J.P., Morffy, N., and Nelson, D.C. (2016). Functional redundancy in the control of
794         seedling growth by the karrikin signaling pathway. Planta 243: 1397–1406.

795    Stanga, J.P., Smith, S.M., Briggs, W.R., and Nelson, D.C. (2013). SUPPRESSOR OF MORE
796         AXILLARY GROWTH2 1 controls seed germination and seedling development in
797         Arabidopsis. Plant Physiol. 163: 318–330.

798    Steiert, F., Petrov, E.P., Schultz, P., Schwille, P., and Weidemann, T. (2018). Photophysical
799         Behavior of mNeonGreen, an Evolutionarily Distant Green Fluorescent Protein. Biophys. J.
800         114: 2419–2431.

801    Stirnberg, P., Furner, I.J., and Ottoline Leyser, H.M. (2007). MAX2 participates in an SCF
802         complex which acts locally at the node to suppress shoot branching. Plant J. 50: 80–94.

803    Stoddard, A. and Rolland, V. (2019). I see the light! Fluorescent proteins suitable for cell
804         wall/apoplast targeting in Nicotiana benthamiana leaves. Plant Direct 3: e00112.

805    Sun, X.-D. and Ni, M. (2011). HYPOSENSITIVE TO LIGHT, an alpha/beta fold protein, acts
806         downstream of ELONGATED HYPOCOTYL 5 to regulate seedling de-etiolation. Mol. Plant
807         4: 116–126.

808    Swarbreck, S.M., Guerringue, Y., Matthus, E., Jamieson, F.J.C., and Davies, J.M. (2019).
809         Impairment in karrikin but not strigolactone sensing enhances root skewing in Arabidopsis
810         thaliana. Plant J. 98: 607–621.

811    Szymczak, A.L. and Vignali, D.A.A. (2005). Development of 2A peptide-based strategies in the
812         design of multicistronic vectors. Expert Opin. Biol. Ther. 5: 627–638.

813    Szymczak, A.L., Workman, C.J., Wang, Y., Vignali, K.M., Dilioglou, S., Vanin, E.F., and Vignali,
814         D.A.A. (2004a). Correction of multi-gene deficiency in vivo using a single "self-cleaving" 2A
815         peptide-based retroviral vector. Nat. Biotechnol. 22: 589–594.

816    Szymczak, A.L., Workman, C.J., Wang, Y., Vignali, K.M., Dilioglou, S., Vanin, E.F., and Vignali,
817         D.A.A. (2004b). Correction of multi-gene deficiency in vivo using a single "self-cleaving" 2A
818         peptide–based retroviral vector. Nature Biotechnology 22: 589–594.

819    Tafreshi, N.K., Sadeghizadeh, M., Emamzadeh, R., Ranjbar, B., Naderi-Manesh, H., and
820         Hosseinkhani, S. (2008). Site-directed mutagenesis of firefly luciferase: implication of
821         conserved residue(s) in bioluminescence emission spectra among firefly luciferases.
822         Biochem. J 412: 27–33.

823    Tailor, R.H., Acland, D.P., Attenborough, S., Cammue, B.P., Evans, I.J., Osborn, R.W., Ray,
824         J.A., Rees, S.B., and Broekaert, W.F. (1997). A novel family of small cysteine-rich
825         antimicrobial peptides from seed of Impatiens balsamina is derived from a single precursor
826         protein. J. Biol. Chem. 272: 24480–24487.

827    Takada, S. and Jürgens, G. (2007). Transcriptional regulation of epidermal cell fate in the
828         Arabidopsis embryo. Development 134: 1141–1150.

829    Tannous, B.A., Kim, D.-E., Fernandez, J.L., Weissleder, R., and Breakefield, X.O. (2005).
830         Codon-optimized Gaussia luciferase cDNA for mammalian gene expression in culture and
831         in vivo. Mol. Ther. 11: 435–443.

832    Thorn, K. (2017). Genetically encoded fluorescent tags. Mol. Biol. Cell 28: 848–857.

833    Urwin, P.E., Zubko, E.I., and Atkinson, H.J. (2002). The biotechnological application and
834        limitation of IRES to deliver multiple defence genes to plant pathogens. Physiological and
835        Molecular Plant Pathology 61: 103–108.

836    Urwin, P., Yi, L., Martin, H., Atkinson, H., and Gilmartin, P.M. (2000). Functional characterization
837        of the EMCV IRES in plants. Plant J. 24: 583–589.

838    Vaucheret, H., Béclin, C., Elmayan, T., Feuerbach, F., Godon, C., Morel, J.-B., Mourrain, P.,
839        Palauqui, J.-C., and Vernhettes, S. (1998). Transgene-induced gene silencing in plants.
840        The Plant Journal 16: 651–659.

841    Villaécija-Aguilar, J.A., Hamon-Josse, M., Carbonnel, S., Kretschmar, A., Schmid, C., Dawid, C.,
842        Bennett, T., and Gutjahr, C. (2019). SMAX1/SMXL2 regulate root and root hair
843        development downstream of KAI2-mediated signalling in Arabidopsis. PLOS Genetics 15:
844        e1008327.

845    Wang, L., Wang, B., Jiang, L., Liu, X., Li, X., Lu, Z., Meng, X., Wang, Y., Smith, S.M., and Li, J.
846        (2015). Strigolactone Signaling in Arabidopsis Regulates Shoot Development by Targeting
847        D53-Like SMXL Repressor Proteins for Ubiquitination and Degradation. Plant Cell 27:
848        3128–3142.

849    Waters, M.T., Nelson, D.C., Scaffidi, A., Flematti, G.R., Sun, Y.K., Dixon, K.W., and Smith, S.M.
850        (2012). Specialisation within the DWARF14 protein family confers distinct responses to
851        karrikins and strigolactones in Arabidopsis. Development 139: 1285–1295.

852    Waters, M.T., Scaffidi, A., Flematti, G., and Smith, S.M. (2015). Substrate-Induced Degradation
853        of the α/β-Fold Hydrolase KARRIKIN INSENSITIVE2 Requires a Functional Catalytic Triad
854        but Is Independent of MAX2. Mol. Plant 8: 814–817.

855    Welsh, J.P., Patel, K.G., Manthiram, K., and Swartz, J.R. (2009). Multiply mutated Gaussia
856        luciferases provide prolonged and intense bioluminescence. Biochem. Biophys. Res.
857        Commun. 389: 563–568.

858    Wend, S., Dal Bosco, C., Kämpf, M.M., Ren, F., Palme, K., Weber, W., Dovzhenko, A., and
859        Zurbriggen, M.D. (2013). A quantitative ratiometric sensor for time-resolved analysis of
860        auxin dynamics. Sci. Rep. 3: 2052.

861    Wood, K.V. (1995). Marker proteins for gene expression. Current Opinion in Biotechnology 6:
862        50–58.

863    Wroblewski, T., Tomczak, A., and Michelmore, R. (2005). Optimization of Agrobacterium-
864        mediated transient assays of gene expression in lettuce, tomato and Arabidopsis. Plant
865        Biotechnol. J. 3: 259–273.

866    Yang, Y., Li, R., and Qi, M. (2000). In vivo analysis of plant promoters and transcription factors
867        by agroinfiltration of tobacco leaves. Plant J. 22: 543–551.

868    Zhang, B., Rapolu, M., Kumar, S., Gupta, M., Liang, Z., Han, Z., Williams, P., and Su, W.W.
869        (2017). Coordinated protein co-expression in plants by harnessing the synergy between an
870        intein and a viral 2A peptide. Plant Biotechnol. J. 15: 718–728.

871   Zhou, F. et al. (2013). D14-SCF(D3)-dependent degradation of D53 regulates strigolactone
872         signalling. Nature 504: 406–410.

873
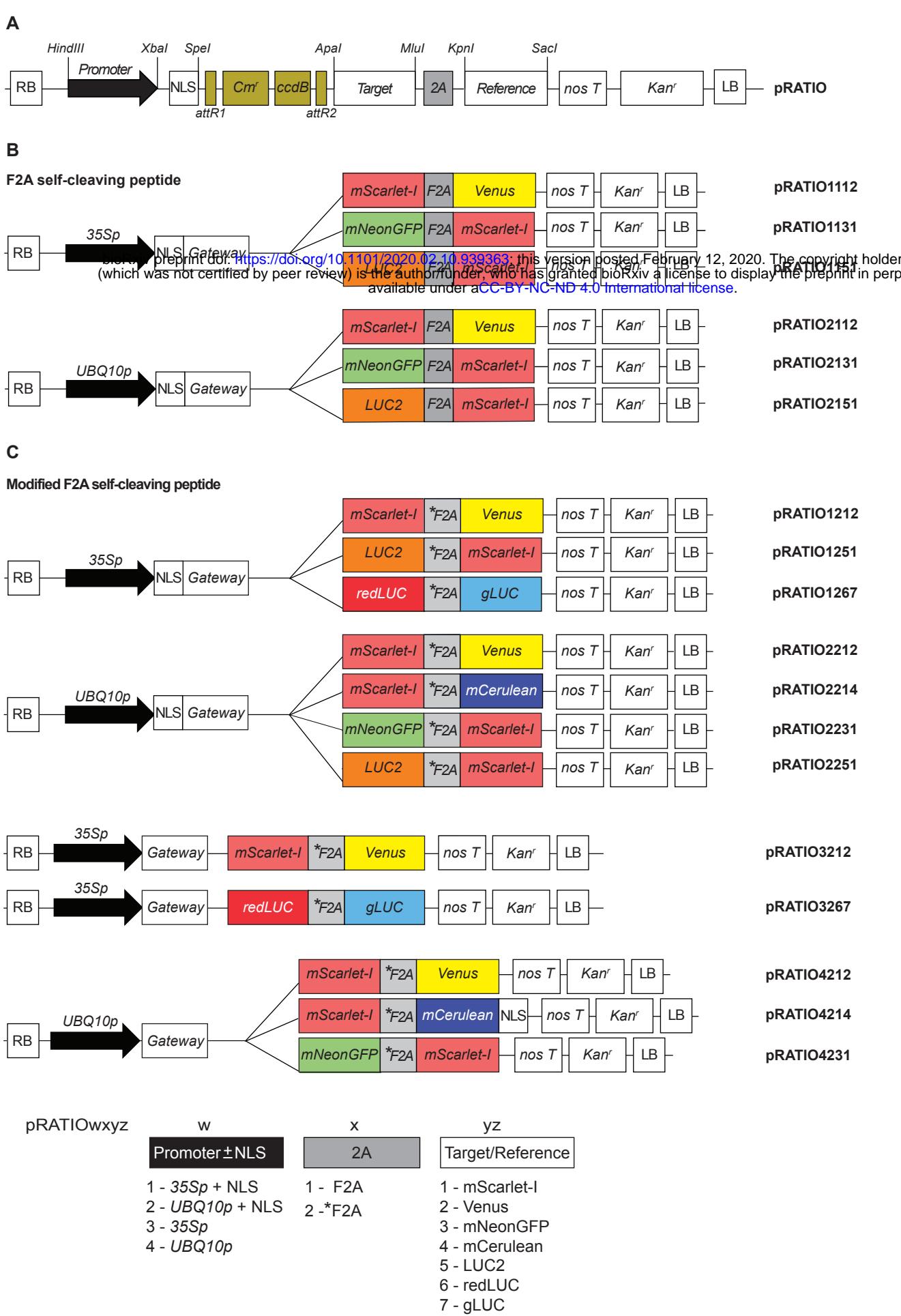
**Figure 1.** Schematic of the pRATIO vector series.

**(A)** General structure of pRATIO vector. Expression is either driven by *CaMV35S* (1000/3000 series) or *UBQ10* promoter (2000/4000 series). Unique restriction sites flank the promoter, NLS, ccdB cassette, target protein, 2A sequence, and the reference protein. The expression cassettes are in pGWB401 or pGWB402 backbones. T-DNA selection is kanamycin resistance.

**(B, C)** pRATIO incorporating either **(B)** F2A self-cleaving peptide or **(C)** modified F2A (*F2A) protein.

LUC2, firefly luciferase; redLUC, red firefly luciferase; gLUC, Gaussia Dura luciferase; RB, right border; LR, left border; Cmr, chloramphenicol-resistance marker (chloramphenicol acetyl transferase) used for selection in bacteria; ccdB, negative selection marker used in the bacteria; nosT, NOS terminator to stop the transcription.

The GenBank accession numbers are listed in Table S5.
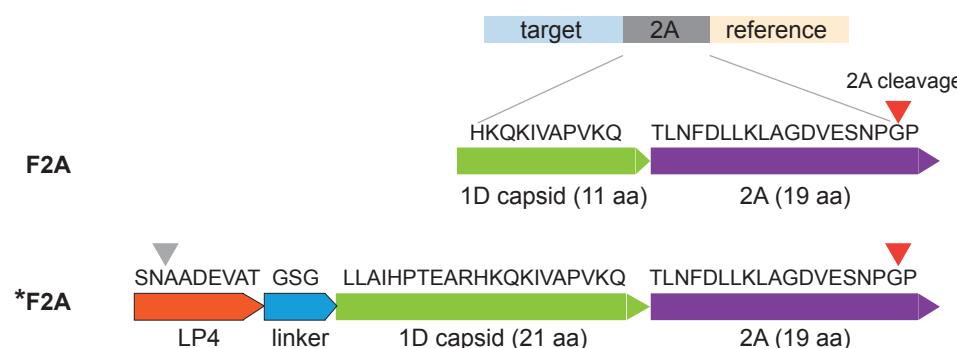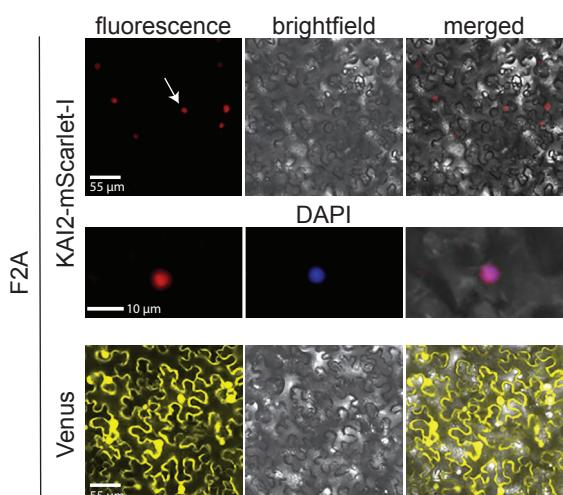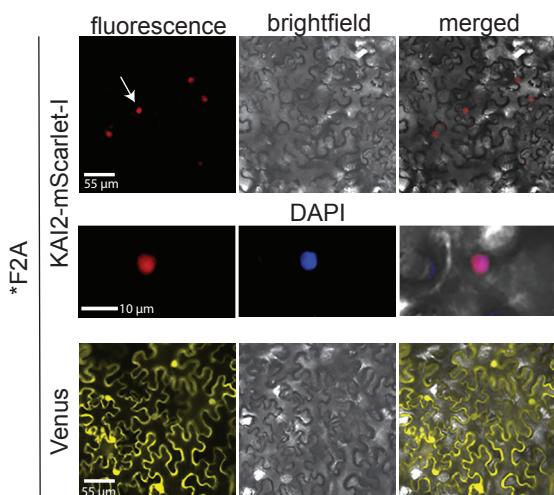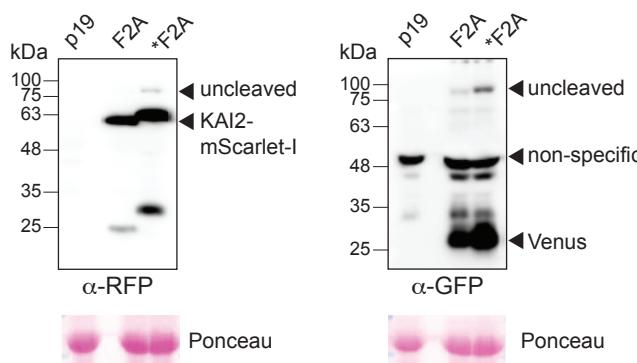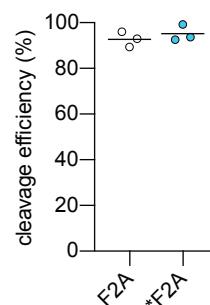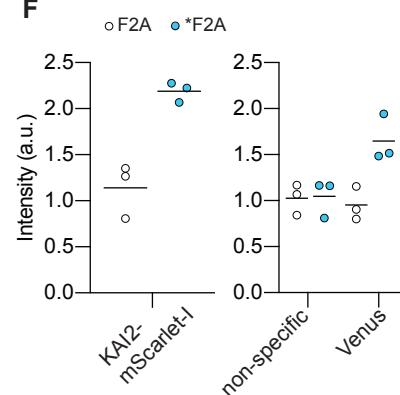
**Figure 2.** Both F2A and *F2A peptides allow the efficient production of two independent polypeptides in tobacco.

**(A)** Amino acid sequences of the two 2As used, foot and mouth disease virus 2A (F2A) and a longer F2A sequence (*F2A). LP4 plant peptide (-SNAADEVAT-) and a GSG linker was added to the N-terminus of *F2A to improve the cleavage efficiency. The site of protease cleavage and 2A mediated cleavage is indicated by green and red arrows, respectively.
**(B, C)** Patterns of localization of mScarlet-I and Venus in *N.benthamiana* epidermal cells expressing
**(B)** pRATIO1112-KAI2 and **(C)** pRATIO1212-KAI2. Venus (yellow) localizes throughout the cells whereas mScarlet-I (red): NLS-KAI2-mScarlet-I remains tightly restricted to the nucleus as expected if they are produced as two independent polypeptides, suggesting that both 2A peptides are correctly split up. Arrows indicate nuclear localization.
**(D)** Western blot analysis of cleavage efficiency of two types of 2A self-cleaving peptides in the tobacco leaf epidermal cells. The cleavage efficiency was assessed using RFP antibody to detect cleaved KAI2-mScarlet-I and the uncleaved KAI2-mScarlet-I-2A-Venus, and GFP antibody to detect cleaved Venus and uncleaved protein. Leaf transformed with p19 served as the control. The Ponceau membrane staining of the most intense band at 55 kDa (presumably Rubisco) was used as a loading control.
**(E)** Quantitation of cleavage efficiency of 2A peptides in tobacco.
Cleavage efficiency = cleaved form/(cleaved form+uncleaved form).The amount of each form was estimated from its band intensity on the Western blot measured by Image Studio Light (LI-COR). Bar indicates mean, n = 3.
**(F)** Comparison of the amount of cleaved proteins between pRATIO1112 (F2A) and pRATIO1212 (*F2A). The amount is estimated as depicted in **(E)**. Bar indicates mean, n = 3.
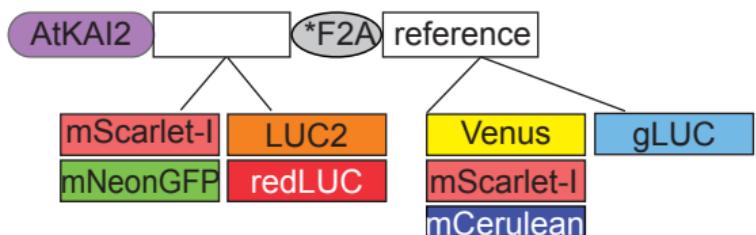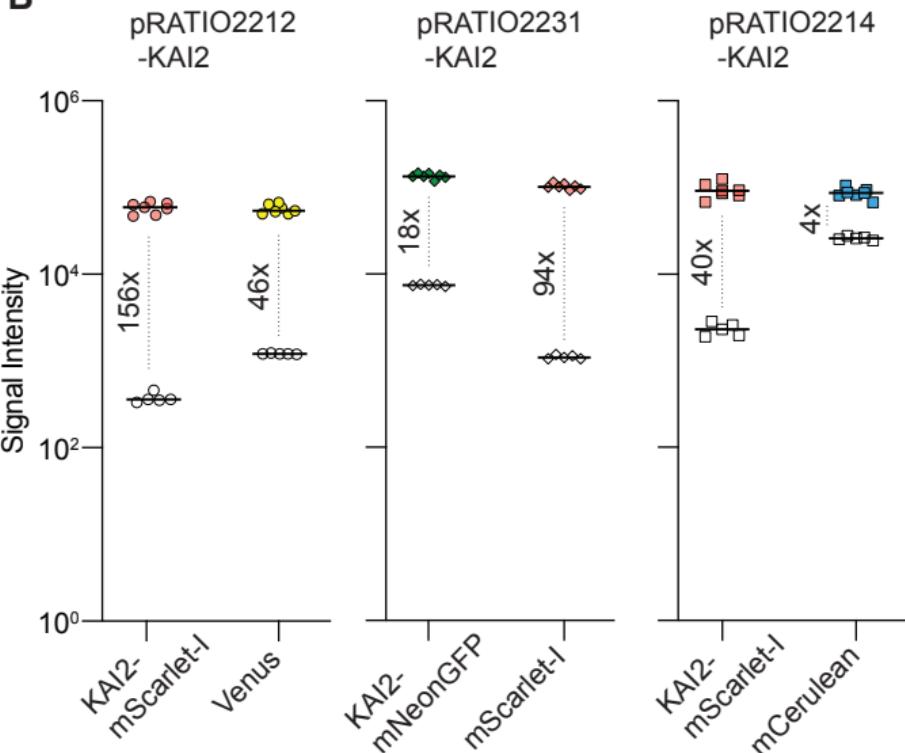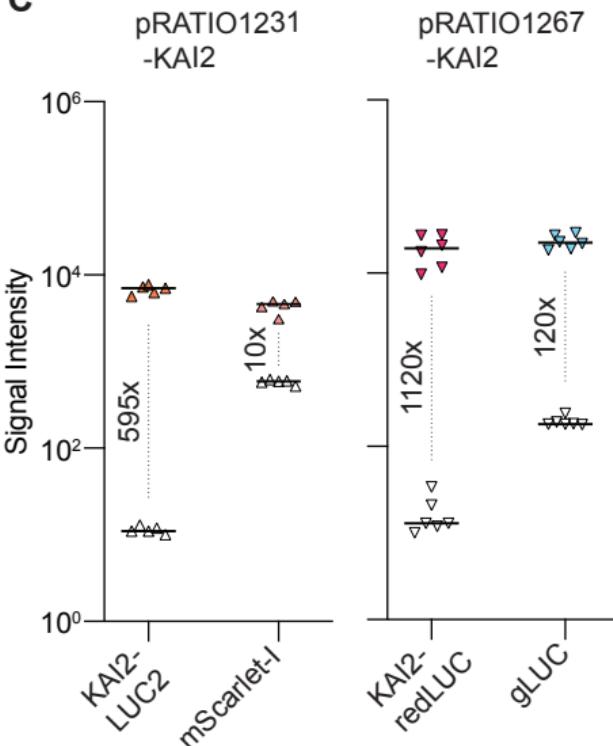
**Figure 3.** Comparison of signal intensity among pRATIO vectors with different combination of target and reference proteins.

**(A)** Schematic of the pRATIO vector expressing Arabidopsis KAI2 cDNA (AtKAI2) fused to different target and reference proteins, **(B, C)** The scatter dot plots comparing signal intensities of the reporter proteins. Leaves transformed with p19 served as the negative control for background signal (open symbols). Fluorescence and luminescence signals were measured in tobacco leaf epidermal cells 72 hpi. Median is shown, n = 4-6 leaf discs. The numbers indicate fold increase in signal intensity over background.
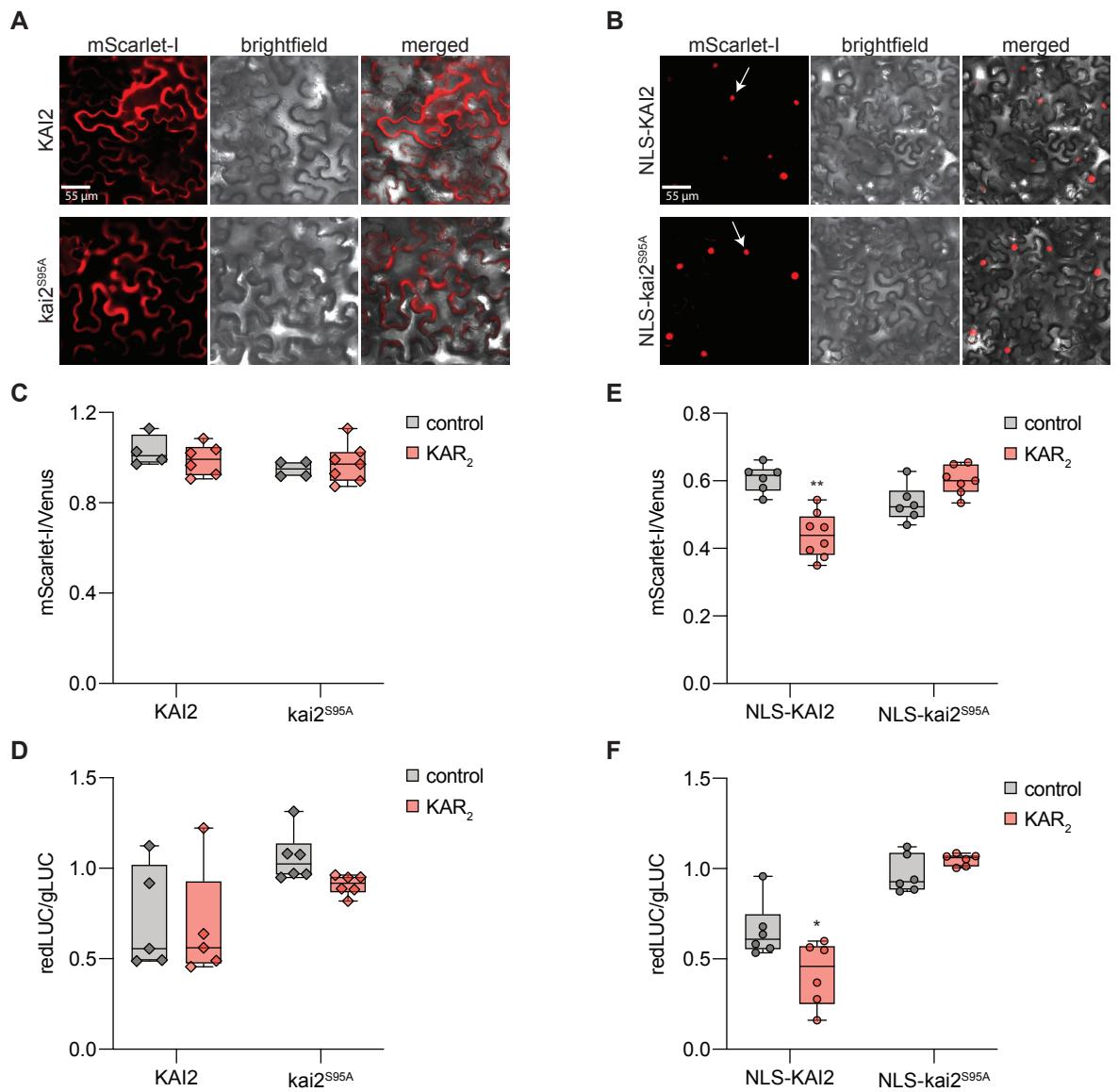
**Figure 4.** Ratiometric detection of KAI2 degradation in tobacco.

**(A, B)** *N.benthamiana* leaf epidermal cells expressing wild type *Arabidopsis* KAI2 (AtKAI2) and catalytically inactive mutant of KAI2 (kai2$^{S95A}$) fused to mScarlet-I in **(A)** pRATIO4212 and **(B)** pRATIO2212. Images were visualized using the RFP epifluorescence settings. Arrows indicate nuclear localization. Scale bar = 55 μm.
**(C-F)** Box and whisker plots showing KAR$_2$ induced degradation response of KAI2 and kai2$^{S95A}$ in transiently transformed tobacco epidermal cells. Degradation response was monitored in **(C, D)** pRATIO4212 and pRATIO3267 (without NLS fusion), **(E, F)** pRATIO2212 and pRATIO1267 (KAI2/*kai2$^{S95A}$* cDNA fused with nuclear localization signal (NLS) at N-terminus in the presence of 10 μM KAR$_2$ or 0.02% acetone control. mScarlet-I-to-Venus (mScarlet-I/Venus) and redLUC-to-gLUC (redLUC/gLUC) ratios are plotted on the y-axis. n = 4-7 leaf discs. * $P < 0.01$; ** $P < 0.001$, Mann-Whitney U test comparisons to control treatment.